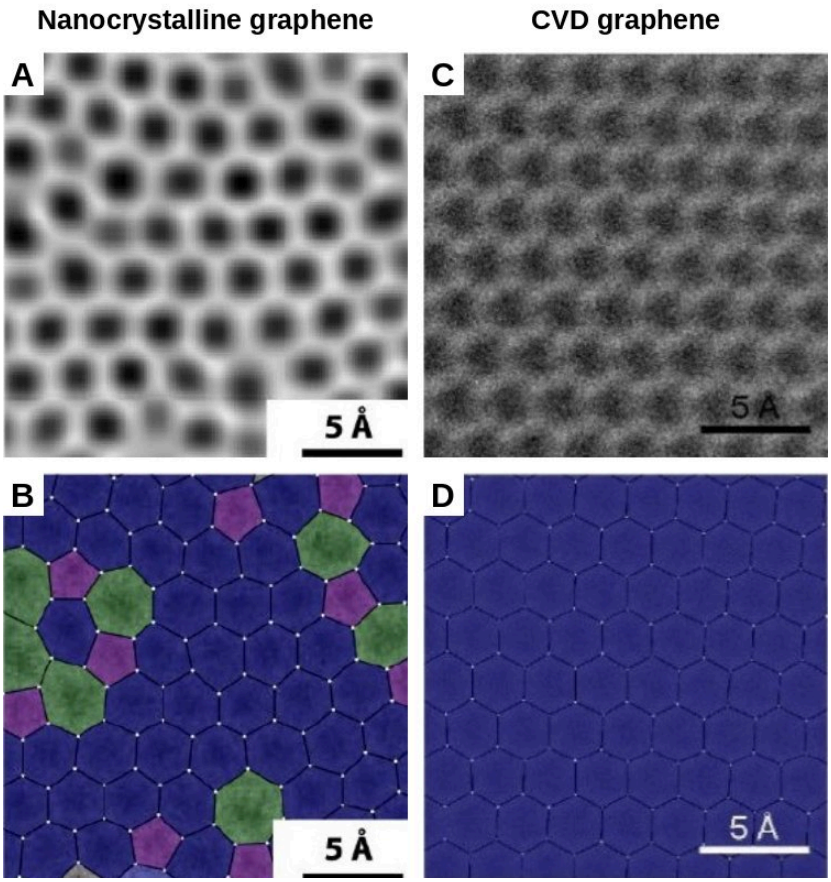

Fig. 1: Nanocrystalline vs. CVD graphene: HRTEM and polygon maps.

Bottom-Up Nanocrystalline Graphene

January 2, 2026 · salve-project.de/newspress/bottom_up_nanocrystalline_graphene.html

January 2, 2026 – Researchers from Leiden University, Ulm University, TU Dresden, TU Darmstadt, the University of Groningen and Xi'an Jiaotong University have developed a bottom-up synthesis method for centimeter-sized nanocrystalline graphene monolayers by pyrolyzing a Langmuir monolayer of a polyaromatic hydrocarbon at the water-air interface. The resulting material is just 0.36 nm thick, comparable to single-layer graphene, and offers a modular strategy for designing nanocrystalline 2D films with potential applications in nanoelectronics and as free-standing membranes. Aberration-corrected HRTEM at 80 kV with the SALVE instrument resolved its grains atom by atom.

A single layer of carbon atoms is usually grown from simple gases such as methane or ethanol, so its structure is set by the furnace – temperature, pressure, flow rates – rather than by the chemistry of the precursor.[1]–[3] The team had earlier made a 2 nm thick amorphous carbon monolayer by pyrolyzing a Langmuir film of a large polyaromatic hydrocarbon whose molecules stand edge-on on water.[4],[5] Now they spread hexa(terpyridine)hexaphenylbenzene (HTPHPB), a polyaromatic hydrocarbon with a less conjugated core, on water, where hydrogen bonds to its pyridine groups make the molecules lie flat. The molecular film was free-standing on a TEM grid even before annealing, held together by its pyridine groups. It was transferred onto a Si wafer and annealed under inert atmosphere at up to 1000 °C. The result is a centimeter-sized carbon film 0.36 nm thick, the thickness of single-layer graphene, that is free-standing over holes of 2 µm.

Atom by atom at 80 kV

Raman spectroscopy and electron diffraction both showed a lack of long-range order: selected-area diffraction, taken at 80 kV with a Thermo Fisher Scientific Talos 200X, has only two diffuse rings, at 4.7 and 8.1 nm^{-1}, as in graphitic carbon. What the film looks like at the atomic level, however, only the microscope can show. Christopher Leist, Haoyuan Qi and Ute Kaiser imaged it at Ulm University with the image-side C_c/C_s-corrected SALVE instrument at 80 kV, whose point resolution is better than 80 pm, so every carbon atom is resolved; the atoms appear bright on a dark background. The AC-HRTEM image of the film annealed at 1000 °C shows nanometer-sized graphene patches embedded in a defective matrix; the small grains are randomly oriented, without long-range order. Magnified, a patch shows the carbon rings (Fig. 1A), while CVD graphene, imaged for comparison, is a regular honeycomb (Fig. 1C).

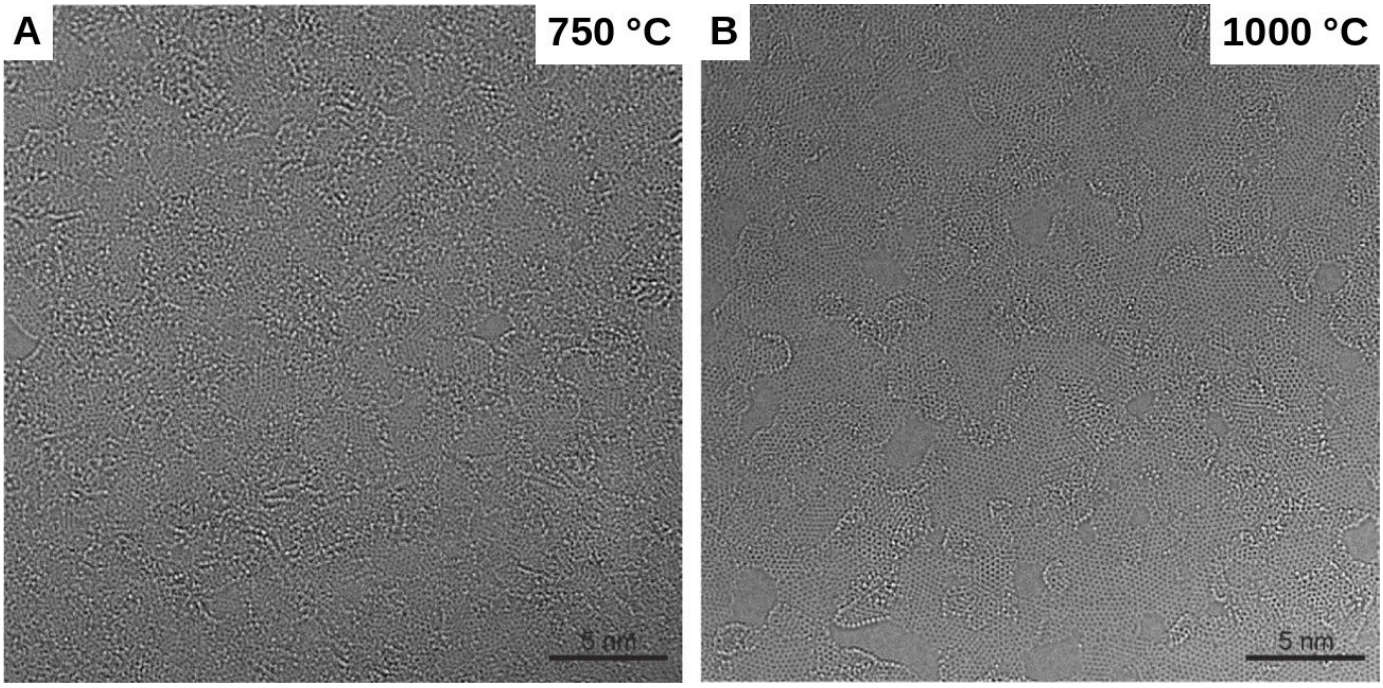

Fig. 2: AC-HRTEM after annealing at 750 °C and 1000 °C.

In such a disordered lattice, bonds and rings cannot be counted by hand. A neural network of the U-Net type located every atom and every ring automatically and excluded regions that were not monolayer, such as contamination or local thickness variations; the team had developed this deep-learning pipeline for amorphous 2D materials,[6] and the box below tells how it was trained. The polygon maps show pentagons (purple) and heptagons (green) scattered among the hexagons (blue) of the nanocrystalline film (Fig. 1B), while CVD graphene is all hexagons (Fig. 1D). Evaluated over 34 AC-HRTEM images of 29 nm × 29 nm, with 6 million bond angles, 4 million bond lengths and 900 000 polygons (in CVD graphene 700 000, 400 000 and 13 000), the full width at half maximum of the bond angle distribution grows from 16.3° in CVD graphene to 24.0°, and that of the bond length distribution from 0.27 Å to 0.39 Å, while the peaks stay at 120° and 1.4 Å, the signature of sp^2 carbon with short-range order. 20 % of the rings are pentagons, 69 % hexagons and 11 % heptagons, compared with 7 %, 84 % and 9 % in CVD graphene, where image aberrations and errors of the algorithm account for the few non-hexagons: pentagons take the place of hexagons, heptagons barely change.

How the atoms were counted

The network learned from simulated images only, so nothing had to be labelled by hand and no selection bias could creep in. Carbon models were built by placing random seed points, dividing the plane into Voronoi cells and putting a carbon atom on each vertex; for the non-monolayer class a continuous graphene layer was added. abTEM[7] simulated their HRTEM images with the experimental pixel size, aberrations, a defocus of 10–50 Å and an electron dose of (1–3) × 10^5 $e^-/Å^2$, plus a random linear intensity gradient that made the network robust against uneven backgrounds.

Four separate networks of a modified U-Net type[8] were trained with 1000 to 4000 images each (512 × 512 pixels for monolayer and vacuum, 256 × 256 pixels for atoms and ring centres): one each for the atom positions, the ring centres, holes in the membrane and non-monolayer regions. Because the experimental images have a wider contrast range than the small training images, they were normalized before evaluation. Atom positions were then read from the network output as the centres of the bright objects.

How the grains form

The annealing temperature decides how far the carbon orders. Comparing films annealed at 750 °C and at 1000 °C, AC-HRTEM shows a larger fraction of monolayer sp^2 regions at the higher temperature, with grains around 2 nm (Fig. 2). The same happened in situ in the microscope: a film crosslinked at 750 °C on a MEMS heating chip was annealed a second time at 550 °C and then at 1000 °C. The same nanocrystalline monolayers later served at Ulm to engineer grain boundaries with the electron beam at 80, 60 and 40 kV. Although the pyridine groups are fully decomposed above 700 °C, the remaining carbon atoms first form a highly disordered layer, an ultrathin carbon reservoir, and only further heating drives them into the crystalline state.

The many grain boundaries also set the film's properties. On the insulating wafer the film is an insulator with a sheet resistance above 10 TΩ sq^{-1}, the highest value reported so far for 2D carbon membranes,[1],[9] and a blue laser etches it away within seconds, whereas pristine graphene survives minutes, because the small grains largely lower the thermal conductivity.[10] The authors conclude that its "atomic thin nature" makes it "potentially useful as a free-standing membrane and in nanoelectronics", and since it grows directly on a Si/SiO_2 wafer and can be patterned by laser, no transfer step is needed before device integration.

Resource

Liu, X., Calvani, D., Leist, C., Makurat, M., Melcrová, A., He, M., Scholma, D., Sevink, G. J. A., Buda, F., Hermans, Y., Hofmann, J. P., Qi, H., Feng, X., Roos, W. H., Kaiser, U., & Schneider, G. F. (2026).
Monolayer nanocrystalline graphene synthesized from pyrolyzing a Langmuir monolayer of a polyaromatic hydrocarbon.
Sci. Adv. **12**(1), eadv1856.
https://doi.org/10.1126/sciadv.adv1856

References

1. Toh, C. T. et al. (2020). Synthesis and Properties of Free-Standing Monolayer Amorphous Carbon. *Nature*, **577**, 199-203. https://doi.org/10.1038/s41586-019-1871-2
2. Dong, J. et al. (2023). Ultrathin Nanocrystalline/Amorphous Carbon Films With Tailored sp^3/sp^2 Bonding Grown by Physical Vapor Deposition. *Carbon*, **213**, 118292. https://doi.org/10.1016/j.carbon.2023.118292
3. Zhou, Y., Loh, K. P. & Lin, J. (2018). Synthesis of Graphene From Acetylene via Chemical Vapor Deposition: Growth Mechanism and Effects of Hydrogen and Carrier Gas. *Carbon*, **126**, 165-175. https://doi.org/10.1016/j.carbon.2017.10.022
4. Liu, X. et al. (2022). Pyrolysis of a Langmuir Monolayer to Molecularly Thin Amorphous Carbon. *Nanoscale*, **14**, 13070-13079. https://doi.org/10.1039/D2NR03206H
5. Liu, X. et al. (2023). In Situ Visualization of Pore Evolution in Monolayer Amorphous Carbon Membranes. *2D Mater.*, **10**, 011001. https://doi.org/10.1088/2053-1583/aca666
6. Leist, C., He, M., Liu, X., Kaiser, U. & Qi, H. (2022). Deep-Learning Pipeline for Statistical Quantification of Amorphous Two-Dimensional Materials. *ACS Nano*, **16**, 20488-20496. https://doi.org/10.1021/acsnano.2c06807
7. Madsen, J. & Susi, T. (2021). The abTEM Code: Transmission Electron Microscopy From First Principles. *Open Res. Europe*, **1**, 24. https://doi.org/10.12688/openreseurope.13015.2
8. Madsen, J., Liu, P., Kling, J., Wagner, J. B., Hansen, T. W., Winther, O. & Schiøtz, J. (2018). A Deep Learning Approach to Identify Local Structures in Atomic-Resolution Transmission Electron Microscopy Images. *Adv. Theory Simul.*, **1**, 1800037. https://doi.org/10.1002/adts.201800037
9. Hong, J.-Y. et al. (2021). Monolayer Nanocrystalline Graphene From a Liquid Precursor. *Nanoscale*, **13**, 12677-12687. https://doi.org/10.1039/D1NR02689J
10. Liu, H. K., Lin, Y. & Luo, S. N. (2014). Grain Boundary Energy and Grain Size Dependences of Thermal Conductivity of Polycrystalline Graphene. *J. Phys. Chem. C*, **118**, 24797-24802. https://doi.org/10.1021/jp508035b